



# Characterization and Validation of Canine P-Glycoprotein-Deficient MDCK II Cell Lines for Efflux Substrate Screening

Dong Ye<sup>1</sup> · Anna Harder<sup>1,2</sup> · Zhizhou Fang<sup>1,3</sup> · Manuel Weinheimer<sup>1</sup> · Loic Laplanche<sup>1</sup> · Mario Mezler<sup>1</sup>

Received: 19 March 2020 / Accepted: 27 July 2020 / Published online: 11 September 2020  
© Springer Science+Business Media, LLC, part of Springer Nature 2020

## ABSTRACT

**Purpose** We characterized three canine P-gp (cP-gp) deficient MDCKII cell lines. Their relevance for identifying efflux transporter substrates and predicting limitation of brain penetration were evaluated. In addition, we discuss how compound selection can be done in drug discovery by using these cell systems.

**Method** hMDR1, hBCRP-transfected, and non-transfected MDCKII ZFN cells (all with knock-down of endogenous cP-gp) were used for measuring permeability and efflux ratios for substrates. The compounds were also tested in MDR1\_Caco-2 and BCRP\_Caco-2, each with a double knock-out of BCRP/MRP2 or MDR1/MRP2 transporters respectively. Efflux results were compared between the MDCK and Caco-2 models. Furthermore, *in vitro* MDR1\_ZFN efflux data were correlated with *in vivo* unbound drug brain-to-plasma partition coefficient ( $K_{p,uu}$ ).

**Results** MDR1 and BCRP substrates are correctly classified and robust transporter affinities with control substrates are shown. Cell passage mildly influenced mRNA levels of transfected transporters, but the transporter activity was proven stable for several years. The MDCK and Caco-2 models were in high consensus classifying same efflux substrates. Approx. 80% of enlisted substances were correctly predicted with the MDR1\_ZFN model for brain penetration.

**Conclusion** cP-gp deficient MDCKII ZFN models are reliable tools to identify MDR1 and BCRP substrates and useful for predicting efflux liability for brain penetration.

**KEY WORDS** Brain penetration · Efflux ratio (ER) · Madin-Darby canine kidney type II (MDCKII) cells · Net efflux ratio (NER) · Zinc finger nucleases (ZFNs)

## ABBREVIATIONS

|                 |  |
|-----------------|--|
| ABC             | ATP-binding cassette                     |
| API             | Active pharmaceutical ingredient         |
| BCRP            | Breast cancer resistance protein         |
| CNS             | Central nervous system                   |
| cP-gp           | Canine P-glycoprotein                    |
| C <sub>pm</sub> | Count per minute                         |
| C <sub>T</sub>  | Cycle threshold                          |
| DMEM            | Dulbecco's modified eagle medium         |
| DMSO            | Dimethyl sulfoxide                       |
| DPBS            | Dulbecco's phosphate buffered saline     |
| EDTA            | Ethylenediaminetetraacetic acid          |
| EMA             | European medicines agency                |
| ER              | Efflux ratio                             |
| FBS             | Fetal bovine serum                       |
| FDA             | U.S. Food and drug administration        |
| GAPDH           | Glyceraldehyde 3-phosphate dehydrogenase |
| HBSS            | Hank's balanced salt solution            |
| MDCK            | Madin-Darby canine kidney                |
| MDR             | Multidrug resistance                     |
| mRNA            | Messenger RNA                            |
| MRP             | Multidrug resistance associated protein  |
| NEA             | Non-essential amino acids                |
| NER             | Net efflux ratio                         |
| OATP            | Organic anion-transporting polypeptide   |
| OCT             | Organic cation transporter               |

✉ Mario Mezler  
mario.mezler@abbvie.com

<sup>1</sup> Drug Metabolism & Pharmacokinetics-Bioanalytics LU, AbbVie Deutschland GmbH & Co KG, Knollstraße 50, 67061 Ludwigshafen, Germany

<sup>2</sup> Current Address: Global Marketing and Sales, B. Braun Melsungen AG, Plant P Pfiesswiesen, 34212 Melsungen, Germany

<sup>3</sup> Current Address: NCE Drug Metabolism & Pharmacokinetics, Merck Healthcare KGaA, Frankfurter Straße 250, 64293 Darmstadt, Germany

|           |   |
|-----------|---|
| $P_{app}$ | Apparent permeability coefficient               |
| RT-PCR    | Reverse transcription-polymerase chain reaction |
| P-gp      | P-glycoprotein                                  |
| WT        | Wild type                                       |
| ZFN       | Zinc finger nuclease                            |

## INTRODUCTION

*In vitro* permeability and transport assays are routinely conducted in pharmaceutical industry to screen and select the most promising drug candidates for clinical development. Cell lines used for such purpose are required to express specific efflux transporters that enable investigation of transporter-mediated drug-drug interactions (DDIs), according to the guideline of the U.S. Food and Drug Administration (FDA) [1]. For that, epithelial cell lines such as Caco-2 and Madin-Darby Canine Kidney (MDCK) cells represent two major cell models widely used for predicting human absorption. Due to comparable classes of efflux transporters expressed across physiological barriers, including P-glycoprotein (P-gp, also known as multidrug resistance protein 1 (MDR1)), breast cancer resistance protein (BCRP), and multidrug resistance-associated proteins (MRPs), Caco-2 and MDCK cells have been used for assessment of DDI liability and applications of predicting transporter-regulated impediment of the blood-brain barrier [2, 3].

Caco-2 cells were derived from human colon adenocarcinoma, which can grow into a confluent and polarized monolayer under expression of tight junction proteins, such as ZO-1, claudin, occludin *etc.* In contrast to the dog-origin MDCK cells, Caco-2 cells possess a wide range of functional human transporter proteins. Besides common efflux transporters (i.e., hMDR1, hBCRP, hMRP2), uptake transporters such as OATP, OCT, SLC21A and SLC22A are also expressed in Caco-2 cells to function in drug absorption and distribution [4]. Caco-2 cells require extensive time in culture (normally ~21 days) to reach full differentiation and expression of transporters, therefore it has been often restricted to their low-throughput applications, i.e., for late stage drug candidate characterization. In addition, due to variable expression of transporters in Caco-2 subpopulations, it is difficult to attribute a distinct property of a compound, e.g. efflux, to a defined transporter type. For that reason, it is possible to genetically knock out pairs of efflux transporters, e.g., MDR1/BCRP, MDR1/MRP2 or BCRP/MRP2, to keep one prominent transporter in Caco-2 for substrate identification. Conveniently, these Caco-2 models are already available from a commercial vendor [5] and therefore provide easy access for our study.

Despite its non-human origin, the MDCK cell line is however advantageous due to its shorter cultivation time, its high

proliferation rate, its predictability of human intestinal absorption as well as brain exposure. Therefore, MDCK cells are a preferred choice for setting up permeability and efflux transporter assays. So far, two sub-types of MDCK cells have been made available from its parental strain NBL-2, namely type I and type II MDCK cells (MDCKI and MDCKII). MDCKI cells were isolated with lower passage parental MDCK cells and characteristic of high transepithelial electrical resistance (TEER) values ( $>4000 \Omega \cdot \text{cm}^2$ ), while MDCKII cells were obtained from higher passage MDCK cells and with instead lower TEER values ( $<300 \Omega \cdot \text{cm}^2$ ) [6]. Despite both stains were reported in literature, MDCKII cells are however considered as a prominent choice in most efflux transporter studies [6].

Recently, different MDCK cell lines have been reported in literature for the prediction of brain penetration, including MDCKI-MDR1 from the National Institutes of Health (NIH) and MDCKII-MDR1 from Netherlands Cancer Institute (NKI; Borst cell line) [7, 8], human MDCKII-LE-BCRP and mouse MDCKII-mBcrp [9], LLC-PK1-MDR1 and MDCK-MDR1 [10]. MDCK-MDR1 was reported as a superior cell model for the quantitative prediction of brain disposition [10], and the NIH MDCKI-MDR1 was previously suggested to predict the brain penetration better than the Borst cell line. Expression levels of transfected transporters and endogenous P-gp activity from selected MDCK models remain to be important factors affecting the eventual data quality.

It is important to note that the MDCK cells described in this work were derived from the Borst cell lines [11]. As mentioned above, one obstacle that hampers the usefulness of MDCK cells as an *in vitro* screening tool in predicting the contribution of efflux transporters into compound exposure and disposition has been the endogenous expression of cP-gp. As cP-gp can confound permeability and efflux studies if it remains functional, the data generated with these cell lines can lead to underestimated evaluation for passive permeability or exaggerated efflux activity for transfected transporters. As a result, false negative or false positive results likely confound data interpretation for source cell lines, such as the Borst or NIH cell models.

Based on those cells, new MDCK cell lines have been generated using genetic modification in order to circumvent the influence of endogenous efflux transporters in cellular studies. In literature, Simoff *et al.* generated a MDCKII cell line with complete knock-out of MDR1 by using CRISPR-Cas9 gene editing technology [12], and Karlgren *et al.* further characterized these cells with transfected hMDR1 in drug efflux studies [13]. Chen *et al.* from Genentech Inc. adopted a similar CRISPR-Cas9 approach and validated cP-gp-free MDCKI cells with overexpression of human P-gp (hP-gp) in permeability and efflux substrate studies [14]. Prior to these experiments, the elimination of endogenous cP-gp was also achieved

by using zinc finger nuclease (ZFNs) technology [11]. ZFNs are sequence-specific zinc finger nucleases (ZFNs) fused with the restriction enzyme *FokI*. Once ZFNs bind to specific genomic DNA sequence (i.e., cP-gp), dimerization of *FokI* is initiated for genome modification. With ZFN transfection, cP-gp “knock-down” experiments were performed by Gartzke *et al.* [11], based on three cell lines originally from the Netherlands Cancer Research Center, including wild type MDCKII and MDCKII cells transfected with hMDR1 (ABCB1) or hBCRP(ABCG2). Following mRNA expression analysis of ABC transporters and functional permeability and efflux assays, these transfected cell lines, namely WT\_ZFN, MDR1\_ZFN, and BCRP\_ZFN have demonstrated drastic knock-down activities from cP-gp [11].

In this report, we aim to evaluate the suitability and reliability of genetically modified MDCKII ZFN cell models in order to strengthen the scientific basis on how compound selection can be achieved for drug discovery in industry. Numerous transporter substrates were used to characterize permeability and efflux transport properties of the model cell lines, and data variability and robustness was further investigated regarding cell passage, and long-term cultivation factors. Two double knock-out Caco-2 cell lines, including a paired deletion of BCRP/MRP2 or MDR1/MRP2 respectively, were also applied for the substrate identification. As a result, compound permeability and efflux transport results were compared between MDCKII ZFN and double knock-out Caco-2 models. Moreover, a correlation of compound properties was performed in between *in vitro* MDCKII ZFN data and *in vivo* mouse data, and we explored if cP-gp deficient MDCKII ZFN models could be useful in predicting efflux transporter-dependent brain penetration. Our results led to a proposed screening process for compound characterization in discovery and development. We developed a decision tree for the use of key efflux parameters for compound selection.

## MATERIALS AND METHODS

### Materials

Unless stated otherwise, all test compounds (substrates and inhibitors) were obtained internally from AbbVie chemical substance management system (Ludwigshafen, Germany). Commercially available compounds were purchased from Sigma-Aldrich (Taufkirchen, Germany). Radiolabeled probe substrates, including [<sup>3</sup>H]-quinidine and [<sup>3</sup>H]-prazosin, were ordered from American Radiolabelled Chemicals Inc. (Missouri, US). Scintillation gel Ultima Gold XR was obtained from PerkinElmer (Rodgau, Germany). Three MDCKII ZFN cell lines used for this study were all available from the internal cell bank in AbbVie Germany. Double knock-out MDR1\_Caco-2 and BCRP\_Caco-2 cell lines were

ordered from Merck Millipore, Germany. Cell culture reagents, e.g., DPBS, trypsin/EDTA, DMEM medium, sodium pyruvate, L-Glutamine, non-essential amino acids and penicillin-streptomycin solution, were all purchased from Thermo Fisher Scientific (St.Leon-Rot, Germany). Fetal bovine serum was obtained from BioChrom GmbH (Berlin, Germany). All plasticwares were internally available in AbbVie Germany.

### Cell Culture

All studied cell lines were cultivated in 75 cm<sup>2</sup> cell culture flasks at 37°C with 5% CO<sub>2</sub>, and passaged every 5–7 days with DMEM medium, supplemented with 10% FBS, 1% NEA, 1% sodium pyruvate, 1% L-Glutamine. For subculture, cells were rinsed with DPBS once and further incubated in DPBS for 10–15 min, subsequently replaced with 2 mL of trypsin/EDTA solution for 10 min at 37°C to detach the cells. Thereafter, trypsin was deactivated by adding 10 mL of medium and cells were harvested by centrifugation at 300 g for 5 min. For cP-gp-deficient MDCKII ZFN cell lines (with transfection of hMDR1 or hBCRP transporter) and wild-type MDCKII ZFN cells (without recombinant efflux transporter expression), cell culture was maintained with a passage number of 25–50. In parallel, two Caco-2 double knock-out cell lines with paired deletion of BCRP/MRP2, MDR1/MRP2 respectively were maintained in the same DMEM medium above but with 1% penicillin-streptomycin.

In transport studies, all cell lines were seeded into 1 μm Millicell® 96-well transwell plate (Merck Millipore, Germany), comprising the insert plate and the feeder plate. The insert well was seeded with 100 μL cell suspension containing 40,000 cells. The feeder tray was filled with 28 mL of medium. For assay usage, MDCKII cell monolayers were maintained for 5 days, while Caco-2 monolayers were grown for 21 days with media change every 2 days. All transwell plates received fresh media change one day before the experiments to prevent cell starvation.

### Quantitative Real-Time PCR

In order to evaluate cell passage effect on the transporter gene expression, lower and higher passaged MDR1\_ZFN (Passage 23 and 35), BCRP\_ZFN (Passage 19 and 33) and WT\_ZFN cells (Passage 16 and 33) were used for RNA extraction. Total RNA was isolated from MDCKII ZFN cells, using RNeasy® Mini Kit from Qiagen (Hilden, Germany) according to the manufacturers protocol. The concentration and purity of RNA was determined at 260/280 nm with a NanoDrop™ 2000 spectrophotometer from Thermo Fisher Scientific (Wilmington, Germany). Total RNA (~1 μg) was reverse-transcribed into cDNA using Transcriptor First Stand cDNA Synthesis Kit from Roche Diagnostics (Mannheim,

Germany). The quantitative Real-Time PCR (qRT-PCR) was performed with specific primers for hMDR1 (Forward: 5'-CCGAACACATTGGAAGGAA; Reverse: 5'-CTTTGCCATCAAGCAGCACA), hBCRP (Forward: 5'-CAGGTCTGTTGGTCAATCTCACA; Reverse: 5'-TCCATATCCTGGAATGCTGAAG). Fifty nanograms of cDNA was amplified by using QuantiFast™ SYBR® Green PCR kit from Qiagen (Hilden, Germany). SYBR Green dye intercalates double-stranded DNA, which is quantifiable by the incremental fluorescence intensity of SYBR Green at Ex/Em wavelengths of 488/522 nm. Non-specific signals during PCR, i.e., from primer DNA, were controlled, after continuous reheating was applied to PCR products for detection of non-specific peak in the melting curve. As a control gene, GAPDH (Glyceraldehyde 3-phosphate dehydrogenase) was measured along with all mRNA samples prepared for qRT-PCR. For quantification of the relative mRNA expression level,  $\Delta\Delta C_t$  was calculated after normalization of  $C_t$  (Cycle Threshold) value of a transporter gene against  $C_t$  of GAPDH, using the following equation:

$$\Delta\Delta C_t = 2^{-[\Delta C_t(\text{Transporter gene}) - \Delta C_t(\text{GAPDH})]} \quad (1)$$

### Permeability Study

Permeability assays were performed with MDCKII or Caco-2 cells in a similar fashion. Test compounds were prepared at 1  $\mu\text{M}$  in transport buffer (HBSS buffer, pH 7.4) containing the monolayer-integrity marker lucifer yellow (80  $\mu\text{M}$ ). The final concentration of DMSO should be no more than 0.5% in compound solution. Transporter inhibitors, including 5  $\mu\text{M}$  LY335979 (for MDR1), 2  $\mu\text{M}$  KO143 (for BCRP), were applied with compounds for transporter substrate identification. Before the assay, culture medium was removed, and the cells were rinsed with transport buffer once. Compound solutions were added to donor compartments, and transport buffer was added to receiver compartments. The permeability was evaluated after 1 h, when samples were collected from both apical and basolateral sides of transwell plates, and then mixed with a quench solution (30% acetonitrile in water) before measurement by LC-MS/MS. To determine compound apparent permeability ( $P_{\text{app}}$ ), the following equation was used:

$$P_{\text{app}} = \frac{\Delta Q}{\Delta t \cdot A \left( \frac{C_1 + C_0}{2} \right)} \quad (2)$$

where  $\Delta Q$  is the amount of compound permeated through the monolayer as determined by the concentration of compound in the receiver well at the end of the experiment,  $\Delta t$  is the incubation time (60 min),  $A$  is the filter surface area (0.11  $\text{cm}^2$ ),  $C_1$  is the measured concentration in the donor well at the end of the experiment,  $C_0$  is the initial compound

concentration. Permeation velocity is expressed as apparent permeability ( $P_{\text{app}}$ ) with the unit of  $10^{-6}$   $\text{cm/s}$ .

The efflux ratio (ER) was obtained according to the following equation:

$$\text{ER} = \frac{P_{\text{app}} \text{ BA}}{P_{\text{app}} \text{ AB}} \quad (3)$$

where  $P_{\text{app}} \text{ AB}$  or  $P_{\text{app}} \text{ BA}$  refers to the mean permeability of three replicates in the direction of apical to basolateral (A-to-B) or basolateral to apical (B-to-A), respectively. If one compound acquires ER value  $\geq 2$ , it is identified as corresponding transporter substrate; If  $\text{ER} < 2$ , then it is not considered as transporter substrate.

Subsequently, net efflux ratio (NER) was calculated with the following equation:

$$\text{NER} = \frac{\text{ER}_{(\text{transfected})}}{\text{ER}_{(\text{wild type})}} \quad (4)$$

where  $\text{ER}_{(\text{transfected})}$  is the efflux ratio of MDCKII ZFN cell lines transfected with hMDR1 or hBCRP transporter respectively,  $\text{ER}_{(\text{wild type})}$  is the efflux ratio of wild type MDCKII ZFN cells without transfected human transporter.

To assess IVIVC for transporter dependent brain availability/impediment the ER in MDR1\_ZFN cells of 46 reference substances were compared with the unbound partition coefficient ( $K_{p,\text{uu}}$ ), which was calculated as following:

$$K_{p,\text{uu}} = \frac{c_b \cdot f_{u_b}}{c_p \cdot f_{u_p}} \quad (5)$$

Where  $\frac{c_b}{c_p}$  is the brain to plasma ratio of the test substance in mice,  $f_{u_b}$  and  $f_{u_p}$  are the unbound fractions in brain tissue and plasma, respectively.

### Apparent $K_m$ - $V_{\text{max}}$ Transport Assay with Radiolabeled Compounds

In addition to permeability studies, apparent Michaelis-Menten constant ( $K_{m,\text{app}}$ ) and maximum net efflux ratio ( $\text{NER}_{\text{max}}$ ) were determined in cell models with  $^3\text{H}$ -labeled probe substances. Quinidine and prazosin were applied to analyze MDR1- and BCRP-dependent efflux transport. In details, stock substrates were prepared in DMSO and further diluted with pH 7.4, HBSS (with 1% 1 M HEPES, 0.2% 1 M NaOH). Compounds were prepared at a maximal concentration of 100  $\mu\text{M}$ . A two-fold dilution from each of those concentrations was prepared. Lucifer yellow was added to a final concentration at 80  $\mu\text{M}$  within these dilution series.  $T = 0$  samples were directly collected at this point from stock solutions. Over 1 h incubation at 37°C, samples were collected every 30 min and mixed with scintillation liquid before measurement of radioactivity (counts per minute, Cpm) on a MicroBeta Plate Counter from

PerkinElmer (Rodgau, Germany). Samples for Lucifer yellow were also collected at the end of the assays and measured in a TECAN Infinite F200 microplate reader (Männedorf, Switzerland) for evaluation of tight junctions.

For calculation of  $K_{m,app}$ , NER-1 was plotted logarithmically against the concentration of a substrate as following. The fitting of the curve was carried out in GraphPad Prism 5 by using the following equation:

$$NER = \text{Minimum} + \frac{\text{Maximum} - \text{Minimum}}{1 + \left(\frac{x}{K_m}\right)^h} \quad (6)$$

where NER is the efflux ratio of MDCKII ZFN cells recombinantly expressing a respective efflux transporter, normalized with non-transfected MDCKII ZFN control cells (WT\_ZFN), “Minimum” is the curve plateau equivalent to fully saturated substrate transport, “Maximum” is the curve plateau equivalent to maximal substrate transport, “X” is the concentration of a substrate and “h” is the hill slope of the fitted curve. The apparent  $K_m$  value is determined by the substrate concentration ( $\mu\text{M}$ ) which correlates with half of the maximum NER-1 value (termed  $NER_{max}$  as “ $V_{max}$ ”) at y-axis of the fitted curve.

## Data Analysis

Unless stated otherwise, each experiment was performed with triplicates, and repeated for three times. Mean values from three experiments were used for final data analysis.

## RESULTS

### Substrate Identification for Efflux Transporters

In order to comprehensively characterize the newly generated cP-gp-reduced MDCKII cell lines, 27 known MDR1 and BCRP substrates were investigated for their efflux activities, by determining the ER of the cell lines overexpressing hMDR1 and hBCRP (MDR1\_ZFN and BCRP\_ZFN, respectively), as well as in the none-transfected control “wild type” cells (WT\_ZFN). Net efflux ratios (NERs) were determined by normalizing the observed ER of the transfected model with the ER of the wild type model (Table I).

Except for diltiazem and sulfasalazine, 25 of 27 compounds were correctly identified as MDR1 and/or BCRP substrates from two MDCKII ZFN cell lines, when compared to the WT\_ZFN model. Twenty one compounds exhibited  $ER > 2$  in the MDR1\_ZFN cell line. In NER analysis, these 21 compounds also retained  $NER > 2$ , which were therefore identified as MDR1 substrates. In the BCRP\_ZFN cell line, 13 compounds exhibited ER values  $> 2$ . Twelve out of these 13 compounds acquired  $NER > 2$ , thus determined as BCRP

substrates. On the other hand, five compounds including fexofenadine, indinavir, irinotecan, saquinavir and vinblastine, were observed with background efflux in WT\_ZFN cell line. However, a majority of all compounds (22 of 27) did not exhibit efflux transport in the wild type MDCKII cells, which indicated that cP-gp activity was drastically reduced.

Although diltiazem was previously reported as a MDR1 substrate in human P-gp transfected LLC-PK1 model [15], such transporter-mediated efflux was not evident in MDR1-MDCKII cells [16]. A low  $ER = 0.7$  was previously reported for diltiazem [17], similar to our data shown here. In addition, the efflux of sulfasalazine, known as a BCRP substrate, was only found significant in Caco-2 ( $ER = 88$ ) but not in MDR-MDCK cells ( $ER = 1.3$ ), according to Wang *et al.* [18].

In analysis of NER, 21 out of 22 compounds previously reported in the literature as MDR1 substrates were successfully validated as such, with  $NER > 2$  displayed for MDR1 transporter. Similar for reported BCRP substrates, 12 out of 13 compounds were identified, with  $NER > 2$  values again. All these demonstrate that NER analysis was generally in line with the outcome of ER analysis, suggesting both parameters can enable interchangeable assessment for efflux transporter substrates and preclude a residual efflux influence from WT\_ZFN cells.

In Table II, NERs of 16 identified substrates, including 8 MDR1 substrates, 3 BCRP substrates and 5 compounds with affinity for both transporters, were further evaluated with or without treatment of MDR1 and BCRP inhibitors (LY335979 and KO143 respectively), in order to demonstrate if the observed efflux could be effectively inhibited in MDR1\_ZFN and BCRP\_ZFN cell lines. As a result, the NER values of all 8 MDR1 substrates (carvedilol, fexofenadine, indinavir, loperamide, lopinavir, nelfinavir, quinidine, verapamil) could be clearly reduced by LY335979. This was contrasted by their negative efflux outcome individually shown in BCRP\_ZFN cells with or without KO143 inhibitor. Also, the same goes for dantrolene, nitrofurantoin and rosuvastatin, that treatment with KO143 led to a clear decrease of their NERs in BCRP\_ZFN cells, compared to their no apparent efflux in MDR1\_ZFN cells with and without LY335979. Moreover, cimetidine, glyburide, imatinib, irinotecan and prazosin were subject to the inhibition of both LY335979 and KO143 and the compound NERs could be largely reduced, suggesting their dual affinities with MDR1 and BCRP transporters.

In order to further characterize the transport capacity of MDCKII ZFN cells, the kinetic parameters for MDR1 or BCRP-mediated efflux activity ( $K_{m,app}$  and  $NER_{max}$ ) were determined in MDR1\_ZFN and BCRP\_ZFN cells (Fig. 1). Quinidine (MDR1 substrate) and prazosin (BCRP-selective substrate) were used as two reference compounds. Their ERs were measured in dependence of the concentrations used in the MDR1\_ZFN and BCRP\_ZFN cells. Normally, the acquired ER and NER are constant ( $ER_{unsat}$  and  $NER_{unsat}$ , respectively) if transporter-mediated efflux is not saturated

**Table 1** Summary of Efflux Ratios (ERs) and Net Efflux Ratios (NERs) from 27 Substrate Compounds Evaluated in hMDR1 and hBCRP-Transfected, Wild Type MDCKII ZFN Cell Lines.

| Compound       | ER   |      |     | NER  |      | Identified as substrate of | Known in literature as substrate of |
|----------------|------|------|-----|------|------|----------------------------|-------------------------------------|
|                | MDR1 | BCRP | WT  | MDR1 | BCRP |                            |                                     |
| Amprenavir     | 43.9 | 1    | 1.3 | 33.8 | 0.8  | MDR1                       | MDR1                                |
| Carvedilol     | 3.5  | 0.6  | 0.7 | 5    | 0.9  | MDR1                       | MDR1                                |
| Cetirizine     | 5.5  | 0.9  | 1   | 5.5  | 0.9  | MDR1                       | MDR1                                |
| Cimetidine     | 2.6  | 5.4  | 0.4 | 6    | 12.6 | MDR1, BCRP                 | MDR1, BCRP                          |
| Dantrolene     | 0.5  | 15.1 | 0.4 | 1.3  | 37.8 | BCRP                       | BCRP                                |
| Diltiazem      | 0.7  | 0.7  | 0.6 | 1.2  | 1.2  | <sup>a</sup> n.d.          | MDR1                                |
| Fexofenadine   | 5.4  | 0.9  | 2.3 | 2.3  | 0.4  | MDR1                       | MDR1                                |
| Flavopiridol   | 1.2  | 12.3 | 0.7 | 1.7  | 17.6 | BCRP                       | BCRP                                |
| Gefitinib      | 2.2  | 4.4  | 0.7 | 3.1  | 6.3  | MDR1, BCRP                 | MDR1, BCRP                          |
| Glyburide      | 13.5 | 36   | 1.1 | 12.3 | 32.7 | MDR1, BCRP                 | MDR1, BCRP                          |
| Imatinib       | 9.8  | 8.2  | 0.7 | 14   | 11.7 | MDR1, BCRP                 | MDR1, BCRP                          |
| Indinavir      | 92.2 | 2.2  | 3.2 | 28.8 | 0.7  | MDR1                       | MDR1                                |
| Irinotecan     | 42.1 | 12.4 | 2.8 | 15   | 4.4  | MDR1, BCRP                 | MDR1, BCRP                          |
| Loperamide     | 26.8 | 1.1  | 0.9 | 29.8 | 1.2  | MDR1                       | MDR1                                |
| Lopinavir      | 73.1 | 0.8  | 0.8 | 91.4 | 1    | MDR1                       | MDR1                                |
| Mitoxantrone   | 19.7 | 14   | 1.2 | 16.4 | 11.7 | MDR1, BCRP                 | MDR1, BCRP                          |
| Naratriptan    | 12.8 | 1.3  | 1.4 | 9.1  | 0.9  | MDR1                       | MDR1                                |
| Nelfinavir     | 82   | 1.1  | 0.9 | 91.1 | 1.2  | MDR1                       | MDR1                                |
| Nitrofurantoin | 0.2  | 3    | 0.2 | 1    | 15   | BCRP                       | BCRP                                |
| Prazosin       | 3    | 10.9 | 0.7 | 4.3  | 15.6 | MDR1, BCRP                 | MDR1, BCRP                          |
| Quinidine      | 29.1 | 0.7  | 0.9 | 32.3 | 0.8  | MDR1                       | MDR1                                |
| Rosuvastatin   | 1.2  | 2.5  | 0.7 | 1.7  | 3.6  | BCRP                       | BCRP                                |
| Saquinavir     | 57   | 1.7  | 9.4 | 6.1  | 0.2  | MDR1                       | MDR1                                |
| SN-38          | 14.7 | 28.2 | 0.6 | 24.5 | 47   | MDR1, BCRP                 | MDR1, BCRP                          |
| Sulfasalazine  | 0.7  | 1.4  | 1.1 | 0.6  | 1.3  | <sup>a</sup> n.d.          | BCRP                                |
| Verapamil      | 4.1  | 1.9  | 1   | 4.1  | 1.9  | MDR1                       | MDR1                                |
| Vinblastine    | 312  | 1.9  | 9.5 | 32.8 | 0.2  | MDR1                       | MDR1                                |

<sup>a</sup> n.d. not determined

[19]. Saturated transporters would consequently lead to ER or NER value close to 1, mainly because the apical-to-basolateral and basolateral-to-apical fluxes would be dominated by passive permeability. In order to determine  $K_{m,app}$ , NER can be plotted against the substrate concentration and fitted using a 4-parameter sigmoidal fit, where the inversion point of the fitted curves marks the  $K_{m,app}$ .

Quinidine was incubated in MDR1\_ZFN and WT\_ZFN cells at concentrations between 1.56–100  $\mu$ M. The concentration-dependent transporter efflux in MDR1\_ZFN cells was clearly shown, and MDR1-mediated quinidine transport could be saturated by increasing its concentrations. In WT\_ZFN cells, however, quinidine was not actively transported and no  $ER \geq 2$  was obtained, suggesting that functional cP-gp activity was not prominent in the wild type cells. By plotting the NER against the substrate concentration, the  $NER_{max}$  was calculated to be 20.4 and the  $K_{m,app}$  was 11.5  $\mu$ M. Treatment of LY335979 (5  $\mu$ M) exerted 95% of inhibition of the ER of quinidine at 1.56  $\mu$ M in MDR1\_ZFN cells. The inhibitory outcome

was similar with the one when MDR1\_ZFN cells were treated with 100  $\mu$ M quinidine, indicating that the quinidine efflux could be fully saturated at 100  $\mu$ M.

Similarly, prazosin was tested as a BCRP-selective substrate and its serial concentrations from 1.56 to 100  $\mu$ M were applied in both BCRP\_ZFN and WT\_ZFN cells. Again, saturable efflux could be observed for prazosin in BCRP\_ZFN cells, where ER values decreased over the increasing concentrations. WT\_ZFN cells showed overall negligible efflux of prazosin ( $ER \leq 1.1$ ), indicating of their absent efflux for prazosin. With the NER and substrate concentration plot,  $NER_{max}$  of 8.0 and  $K_{m,app}$  of 9.6  $\mu$ M were calculated. Inhibition with 2  $\mu$ M KO143 eliminated 90% of BCRP-mediated efflux for prazosin at 1.56  $\mu$ M.

### Cell-Passage Effect on Transporter Expression and Efflux Activity

It was reported that human gene-transfected MDCK cells may undergo loss of the cDNA over long-term culture, and

**Table II** NERs of MDR1 and BCRP Substrates with or without Treatment of Selective Inhibitors for hMDR1 and hBCRP-Transfected MDCKII ZFN Cell Lines. LY335979 and KO143 are Inhibitors for hMDR1 and hBCRP Transporters Respectively.

| Compound       | MDR1 substrate | BCRP substrate | NER      |                     |          |                  |
|----------------|----------------|----------------|----------|---------------------|----------|------------------|
|                |                |                | MDR1_ZFN | MDR1_ZFN + LY335979 | BCRP_ZFN | BCRP_ZFN + KO143 |
| Carvedilol     | ✓              | –              | 5        | 0.7                 | 0.9      | 1.1              |
| Fexofenadine   | ✓              | –              | 2.3      | 0.7                 | 0.4      | 0.5              |
| Indinavir      | ✓              | –              | 28.8     | 2.3                 | 0.7      | 0.5              |
| Loperamide     | ✓              | –              | 29.8     | 2.3                 | 1.2      | 1.0              |
| Lopinavir      | ✓              | –              | 91.4     | 2.4                 | 1.0      | 0.8              |
| Nelfinavir     | ✓              | –              | 91.1     | 6.8                 | 1.2      | 0.8              |
| Quinidine      | ✓              | –              | 32.3     | 1.9                 | 0.8      | 0.7              |
| Verapamil      | ✓              | –              | 4.1      | 1                   | 1.9      | 0.9              |
| Dantrolene     | –              | ✓              | 1.3      | 1.0                 | 37.8     | 1                |
| Nitrofurantoin | –              | ✓              | 1.0      | 1.0                 | 15       | 1.5              |
| Rosuvastatin   | –              | ✓              | 1.7      | 1.1                 | 3.6      | 1                |
| Cimetidine     | ✓              | ✓              | 6        | 3.5                 | 12.6     | 2.3              |
| Glyburide      | ✓              | ✓              | 11.9     | 1.6                 | 31.7     | 2.9              |
| Imatinib       | ✓              | ✓              | 14       | 1.3                 | 11.7     | 1                |
| Irinotecan     | ✓              | ✓              | 14.9     | 3.5                 | 4.4      | 0.7              |
| Prazosin       | ✓              | ✓              | 4.3      | 3.1                 | 15.6     | 0.6              |

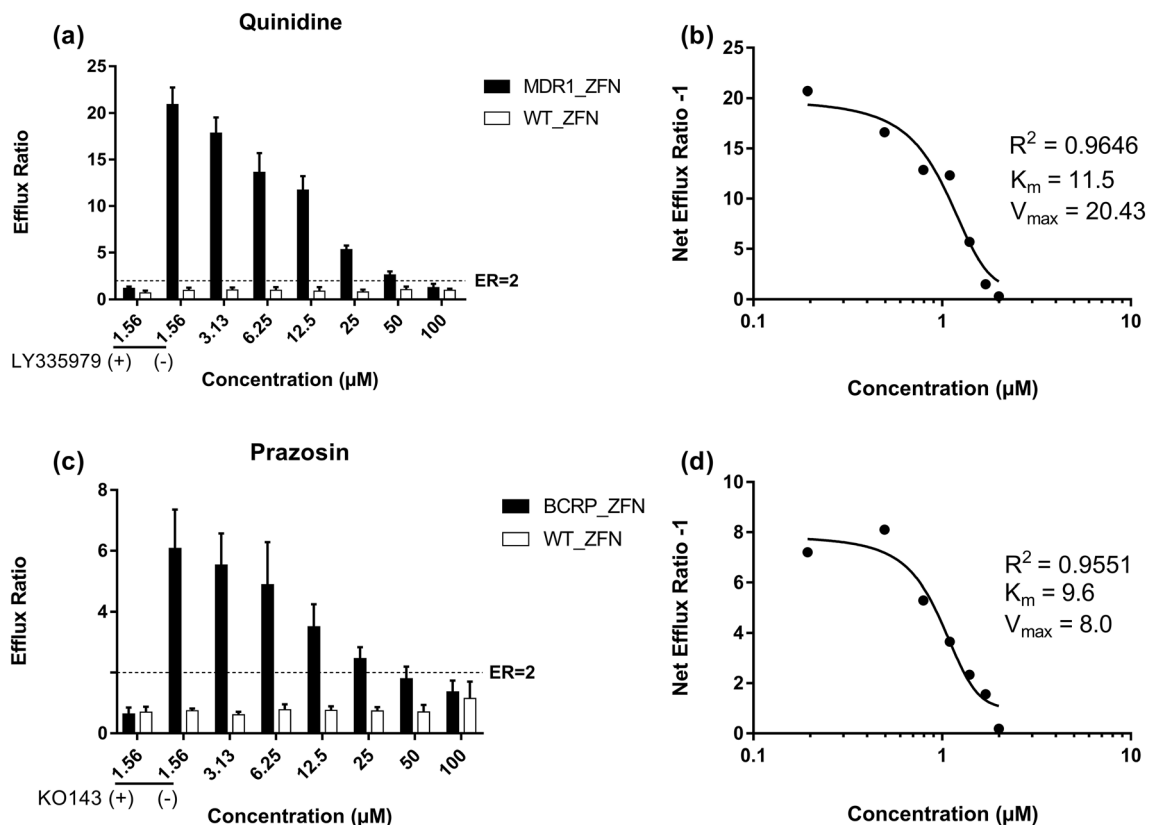


**Fig. 1** Quinidine and prazosin studied with different concentrations in MDR1\_ZFN, BCRP\_ZFN and WT\_ZFN cell lines. ERs from MDR1\_ZFN and WT\_ZFN and their comparison over the increasing quinidine (a) or prazosin (c) concentrations. NERs were calculated with respective ERs, and the curve fitting was obtained by plotting the NERs against quinidine (b) or prazosin (d) concentrations for  $K_{m,app}$  and  $NER_{max}$ . As controls, LY335979 and KO143 inhibitors were used to evaluate MDR1 or BCRP-mediated transport for quinidine and prazosin, respectively

transporter expression was associated with cell passage number [20]. Higher passage cells were assumed to have a lower level of gene expression than lower passage cells, because cell division may exert a “diluting” effect for transfected genes in cell population [20]. In order to characterize these cellular properties, we assessed the passage-dependent effects on transfected hMDR1 and hBCRP efflux activities.

In Fig. 2a and b, relative mRNA expression was assessed with qRT-PCR, and the comparison was drawn among MDR1\_ZFN, BCRP\_ZFN and WT\_ZFN cells for the transfected hMDR1 and hBCRP genes. As expected, hMDR1 gene was dominantly expressed in MDR1\_ZFN cells but found negligible in BCRP\_ZFN and WT\_ZFN cells. Same goes to hBCRP, whose expression was much higher in BCRP\_ZFN cells, compared to MDR1\_ZFN or WT\_ZFN cells. At mRNA expression levels,  $\Delta\Delta C_t$  of hMDR1-transfected MDCKII ZFN cells was 0.95 for Passage 23, compared to  $\Delta\Delta C_t = 1.33$  for Passage 35. Additionally,  $\Delta\Delta C_t$  of hBCRP-transfected MDCKII ZFN cells at Passage 19 was 0.11, compared to  $\Delta\Delta C_t = 0.20$  at Passage 33. That indicates that transfected gene expression from MDCKII ZFN cell models underwent incremental change over continuous cell proliferation, however, such difference remains small and is not distinguished by an order of magnitude. Furthermore, transporter efficiency was also investigated with dependence of cell passage numbers. In Fig. 2c, LY335979 successfully blocked efflux activity of MDR1\_ZFN cells, confirming the role of hMDR1 in efflux of quinidine. Quinidine was studied for MDR1-mediated efflux in MDR1\_ZFN cells at Passage 22, 28, 29, 30 and 33, and their ERs were varied by the passages. However, the maximal ER variation was seen less than 2-fold in between passage 22 and 29. In Fig. 2d, KO143 completely inhibited BCRP\_ZFN, indicating hBCRP was responsible for the efflux of prazosin. ERs of prazosin were evaluated with dependence of cell passages, and passage 18 and 26 showed approx. 2.4-fold, the biggest difference among all passages. With all that, cell-passage dependent effect was shown to mildly affect mRNA expression levels of transfected hMDR1 and hBCRP transporter genes as well as to lead to limited variations of their efflux transport activities. However, it is important to mention that neither hMDR1 nor hBCRP transporter showed the diminishing of efflux activity over continuous passaging of the respective MDCKII ZFN model, as quinidine and prazosin were all identified as efflux substrates as accounted with ERs > 2 throughout. In addition, due to these findings, the numbers of cell passages used in our screening assays were limited within 25–50 to avoid stronger changes in the functional efflux activity. This additional measure ensures stable assessment of efflux liability, as well as cellular permeability.

### Long-Term Stability of Efflux Transporter Activity

The consistent functionalities of transfected efflux transporter proteins are important for MDCKII ZFN cell models

to reliably assess their interactions with new drug candidates. For that reason, ERs of quinidine (MDR1) and prazosin (BCRP) have been routinely measured in periodic assays for the past few years in order to assess the influence of assay conditions (i.e., cell batches, storage, passages, cultivation) and to control the validity of individual permeability and efflux transport assays. In Fig. 3, the long-term efflux results are presented to articulate the ER values obtained for the quality control substrates in MDCKII ZFN models. For MDR1\_ZFN assays (2015–2020), the mean quinidine ER was  $19.38 \pm 7.5$ ; For BCRP\_ZFN assays (2013–2019), the mean prazosin ER was  $6.8 \pm 2.3$ . Respectively, quinidine and prazosin exhibited ER  $\geq 10$  and ER  $\geq 4$  in most of MDR1 or BCRP-dependent assays, indicating that MDR1 and BCRP transporter expression and functionality were consistently maintained throughout several years of MDCKII ZFN assay applications. ER  $\geq 10$  or ER  $\geq 4$  value was therefore used as our quinidine or prazosin qualifier to approve validity of assays for our models. On the other hand, prazosin and quinidine were also counter-measured in MDR1\_ZFN and BCRP\_ZFN respectively, where the ER of prazosin was mostly between 2 to 4 and the ER of quinidine was generally below 2. Because prazosin was previously identified as an MDR1 substrate, so the efflux level was expected. Overall, it suggests that hMDR1 and hBCRP-transfected MDCKII ZFN cell lines are reliable models to maintain a long-term stability for efflux transporter activities, and suitable tools to perform industrial drug screening activities.

### Comparison Between the Caco-2 and MDCKII ZFN Models

The merit of transfecting MDCKII cells with human transporter genes, while leaving cP-gp drastically knocked down, provides a solution to address the model shortcoming upon the species difference, as heterogeneous MDCK wild type cell lines could be varying on transporter expression, thus being misleading for the human situation [21]. The Caco-2 model is well-known for its useful permeability-based prediction for human absorption, thus serves as a valuable reference model to compare the performance of hMDR1 and hBCRP-transfected MDCKII ZFN cells. For that reason, MDR1\_Caco-2 and BCRP\_Caco-2 cell lines were generated via a double knock-out of BCRP/MRP2 and MDR1/MRP2 transporters respectively. Each Caco-2 model contains one prominent efflux transporter (MDR1 or BCRP) to explore the association of a substrate compound with a defined transporter.

In Fig. 4, selected reference compounds were evaluated in the genetically modified Caco-2 and MDCKII ZFN cells. Here, metoprolol was included as a negative control for its passive transport property. Its ERs were ubiquitously at  $\leq 1$  in all Caco-2 and MDCKII ZFN cell lines shown in Fig. 4a and b. Amprenavir and vinblastine exhibited ER values >2 in both



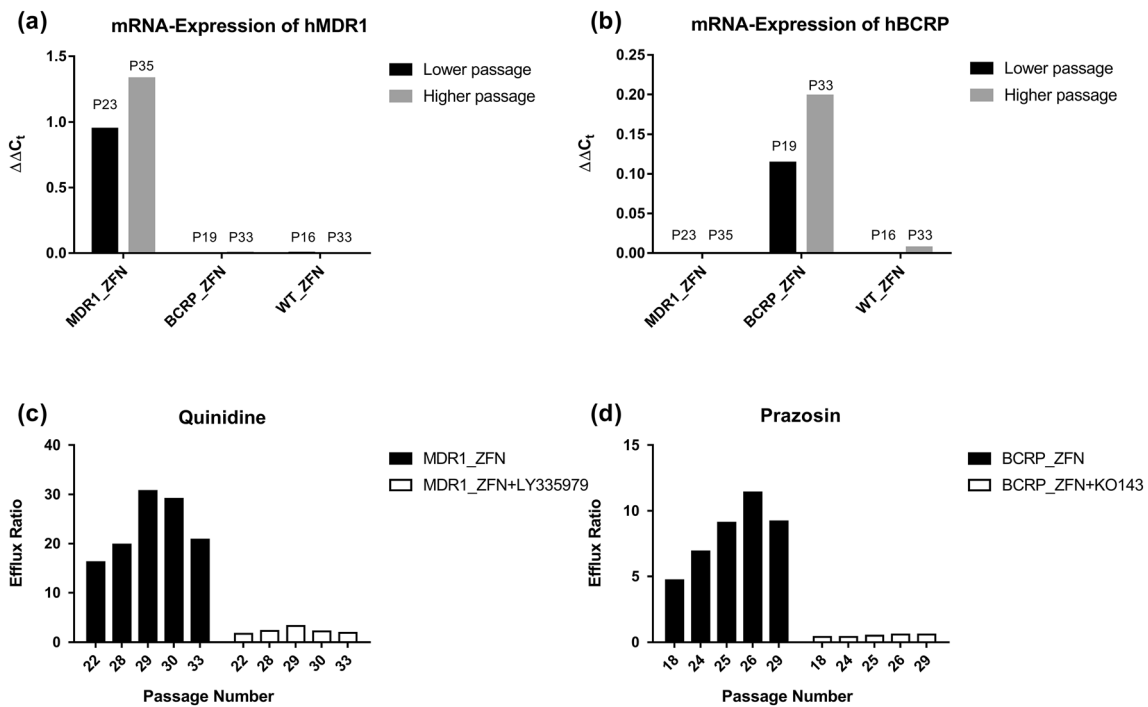


**Fig. 2** mRNA expression and efflux activity of transfected human transporters in MDCK ZFN cells with different passage numbers. With WT\_ZFN cells as a control, lower and higher passages of MDR1\_ZFN and BCRP\_ZFN cells were evaluated and compared over relative mRNA expression of hMDR1 (a) and hBCRP (b) with qRT-PCR. ERs of quinidine (c) or prazosin (d) were compared across different passage numbers of MDR1\_ZFN cells or BCRP\_ZFN cells respectively. Co-treatment of LY335979 or KO143 was applied with the respective cell line as negative control

MDR1\_Caco-2 and MDR1\_ZFN MDCKII cells, as compared to ER <2 seen in BCRP\_Caco-2 and BCRP\_ZFN MDCKII cells. These two compounds were both identified as MDR1 substrates. On the contrary, dantrolene was classified as a substrate in BCRP\_Caco-2 and BCRP\_ZFN MDCKII, but not in the MDR1\_Caco-2 and MDR1\_ZFN MDCKII cells. The ER of dantrolene in BCRP\_Caco-2 was 5-fold higher than in BCRP\_ZFN MDCKII cells. Additionally, cimetidine and nitrofurantoin were identified as BCRP substrates in both BCRP\_Caco-2 and BCRP\_ZFN MDCKII. Fexofenadine was however not identified as such (ER <2), even though its ERs were comparable in the BCRP-dependent Caco-2 and MDCKII ZFN cells.

Different outcomes were observed for rosuvastatin and sulfasalazine when tested in the two different cell systems. In MDR1\_Caco-2 and BCRP\_Caco-2, rosuvastatin showed consistently higher efflux activity (ER = 27.8 and 24, respectively), as compared to the lower ERs in MDR1\_ZFN and BCRP\_ZFN MDCKII (ER = 1.2 and 2.5, respectively). Thus, rosuvastatin could be identified as a dual substrate for both MDR1 and BCRP in the Caco-2 models, while only a substrate in the BCRP\_ZFN MDCKII. In addition, ERs of sulfasalazine in MDR1\_Caco-2 (ER = 4.5) and BCRP\_Caco-2 (ER = 298) were higher than in MDR1\_ZFN (ER = 0.7) and BCRP\_ZFN (ER = 1.4) MDCK II cells, showing approx. 6 and 213-fold differences respectively. Here, the fact that sulfasalazine was

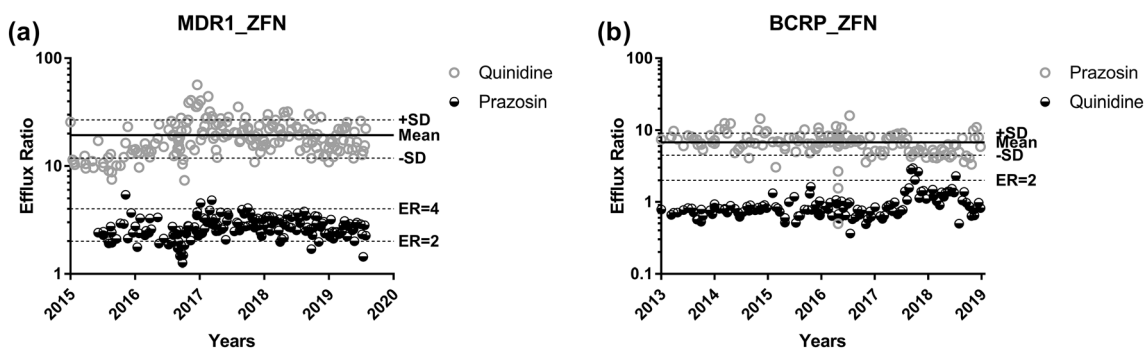


**Fig. 3** Long-term assay overview for ERs of quinidine and prazosin measured in MDR1\_ZFN and BCRP\_ZFN cell models. The qualifier values are ER = 10 and ER = 4 for quinidine and prazosin respectively, where an assay is considered valid if the acquired ER is above the qualifier. ER = 2 is a general ER cut-off value used for identification of efflux transporter substrates

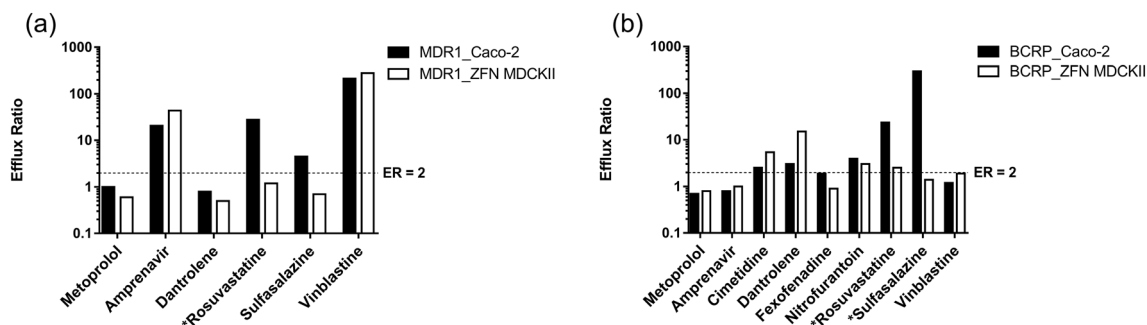


**Fig. 4** Comparison of ERs for a selection of reference compounds measured in double knock-out Caco-2 and transfected MDCKII ZFN cells. In (a) and (b), the asterisk (\*) indicates the ERs of a compound were distinguished by a difference of  $\geq 1$  order of magnitude between the Caco-2 and MDCKII ZFN models

not identified as a substrate of MDR1 or BCRP in our MDCKII ZFN models was also confirmed in the NIH MDR-MDCK cells, where neither MDR1 nor BCRP were reportedly responsible for mediating efflux of sulfasalazine [18].

In summary, a majority of MDR1 and BCRP substrates could be identified in both “knock-out” Caco-2 and “knock-in” MDCKII ZFN cells. MDR1 or BCRP-mediated efflux transport was found with a good degree of agreement in between the transporter-dependent Caco-2 and MDCKII ZFN cell models.

### Robust Predictability for Brain Penetration

The unbound brain to plasma partition coefficient  $K_{p,uu}$  is an important value to assess *in vivo* brain availability and impediment. Through our internal validation, a substance permeating across the blood-brain barrier *in vivo* is generally considered as brain penetrant if  $K_{p,uu} \geq 0.33$ . Here, we used internal and external  $K_{p,uu}$  data of 46 reference compounds from mouse studies and correlated them with their ERs from MDR1\_ZFN MDCKII assays. Results were summarized in Table III, and the correlation between the *in vitro* and *in vivo* data was subsequently performed as in Fig. 5. The plot was divided into four quadrants by using the benchmark values of  $K_{p,uu} = 0.33$  and  $ER = 2$ . In detail, true positive and true negative brain penetration were classified into the quadrants by  $K_{p,uu} \geq 0.33$ ,  $ER < 2$ , and  $K_{p,uu} < 0.33$ ,  $ER \geq 2$ , respectively. In contrast, the quadrants with  $K_{p,uu} < 0.33$ ,  $ER < 2$  and  $K_{p,uu} \geq 0.33$ ,  $ER \geq 2$  represented the false positive and the false negative results, respectively. Using MDR1\_ZFN model, a total 16 compounds were predicted for true positive brain penetration, while 21 compounds were predicted true negatives. In the end, total 37 out of 46 compounds (or 80%) were predicted for their brain penetration outcome, displaying a high predictability from the MDR1\_ZFN MDCKII model.

## DISCUSSION

This study characterized and validated cP-gp-deficient MDCKII cells, which were previously generated with zinc

finger nucleases and transfection of hMDR1 and hBCRP [11]. We demonstrated that these models were reliable to identify substrate compounds for respective transporters, as described in Table I. Overall, 25 out of 27 compounds were identified as MDR1 and/or BCRP substrates in the MDCKII ZFN cells, in agreement with the literature.

For WT\_ZFN MDCKII, 5 MDR1 substrates out of 27 test compounds, including fexofenadine, indinavir, irinotecan, saquinavir and vinblastine, exhibited  $ER > 2$ , suggesting that the background cP-gp transporter or other undesigned transporters remained active. This was however in line with Gartzke *et al.* [11], who reported that cP-gp expression was drastically reduced but not fully eliminated in the MDCKII ZFN models. After all, a majority of MDR1 substrates ( $\sim$  total 16 of 27) did not show efflux activity in WT\_ZFN MDCKII cells, such cP-gp activity was therefore regarded as background effect. Moreover, for indinavir, its ER in WT\_ZFN was 3.2 as compared to 2.3 in BCRP\_ZFN. It further demonstrated the necessity of using NER as the additional parameter to cancel background effect of cP-gp or other undesigned transporters, otherwise false classification of transporters will be generated from measured transporter activity.

In cases of diltiazem and sulfasalazine, the two compounds were not classified as efflux substrates in our two MDCKII ZFN models, based on the calculated ER and NER values (all less than 2). Diltiazem and sulfasalazine were previously known for their heterogenous efflux profiles in MDCKII models, despite they were previously reported as MDR1 and BCRP substrates in other models [15, 18]. Their displayed  $ER < 2$  values in our MDR1\_ZFN or BCRP\_ZFN were in line with other MDCK cell studies [17, 18]. Further, MDR1 and BCRP-mediated efflux properties in MDCKII ZFN cells were evaluated in LY335979 and KO143 inhibition studies (Table II), using 16 substrates selected from Table I. These substrates, with known affinities for either one or two transporters (MDR1 and BCRP) in MDCKII ZFN cells, were again confirmed according to the acquired NERs. Moreover, efflux transport kinetic studies of quinidine and prazosin were performed with a concentration dependence, and their  $K_{m,app}$  values were determined in order to characterize MDR1 and BCRP-mediated transport

**Table III** Data Summary for the Unbound Drug Brain to Plasma Partition Coefficient  $K_{p,uu}$  *In Vivo* and the ERs of MDRI\_ZFN Cells from 46 Reference Compounds.

| Compound         | $K_{p,uu}$           | ER (MDRI_ZFN) |
|------------------|----------------------|---------------|
| Amprenavir       | 0.09                 | 43.9          |
| Bupropion*       | 1.29                 | 0.50          |
| Caffeine*        | 0.46                 | 0.40          |
| Carbamazepine*   | 0.27                 | 0.87          |
| Cetirizine       | 0.01                 | 5.5           |
| Chlorpromazine*  | 0.49                 | 2.40          |
| Cimetidine       | 0.02                 | 2.6           |
| Citalopram*      | 0.68                 | 1.90          |
| Clozapine*       | 1.01                 | 1.12          |
| Cyclobenzaprine* | 1.62                 | 0.90          |
| Desloratadine    | 0.13                 | 22.00         |
| Digoxin          | 0.0038 <sup>a</sup>  | 3.40          |
| Diphenhydramine* | 1.58                 | 0.60          |
| Doxorubicin      | 0.00005 <sup>b</sup> | 13.20         |
| Eletriptan       | 0.06 <sup>c</sup>    | 22.20         |
| Fexofenadine     | 0.04                 | 5.4           |
| Fluvoxamine*     | 1.32                 | 3.52          |
| Haloperidol*     | 1.06                 | 0.80          |
| Hydroxyzine*     | 0.86                 | 0.60          |
| Indinavir        | 0.14                 | 92.2          |
| Ivermectin       | 0.00035 <sup>d</sup> | 0.50          |
| Lamotrigine*     | 0.64                 | 0.60          |
| Loperamide       | 0.02                 | 26.8          |
| Loratadine       | 0.63                 | 0.70          |
| Metoclopramide*  | 0.52                 | 1.30          |
| Naratriptan      | 0.17 <sup>c</sup>    | 12.8          |
| Nelfinavir       | 0.05                 | 82            |
| Nortriptyline*   | 1.63                 | 0.90          |
| Paclitaxel       | 0.07 <sup>e</sup>    | 53.50         |
| Paroxetine*      | 0.86                 | 1.21          |
| Phenytoin*       | 0.28                 | 0.70          |
| Prazosin         | 0.23                 | 3             |
| Quinidine        | 0.05 <sup>f</sup>    | 29.1          |
| Ranitidine       | 0.02                 | 0.59          |
| Risperidone*     | 0.25                 | 6.12          |
| Ritonavir        | 0.67                 | 47.60         |
| Rizatriptan      | 0.11 <sup>c</sup>    | 2.50          |
| Saquinavir       | 0.57                 | 73.40         |
| Selegiline*      | 1.30                 | 0.60          |
| Sulpiride*       | 0.06                 | 2.47          |
| Sumatriptan      | 0.07 <sup>c</sup>    | 2.02          |
| Tripolidine      | 1.75                 | 0.80          |
| Venlafaxine*     | 0.98                 | 0.70          |
| Verapamil        | 0.13 <sup>g</sup>    | 4.1           |

**Table III (continued)**

| Compound     | $K_{p,uu}$        | ER (MDRI_ZFN) |
|--------------|-------------------|---------------|
| Vinblastine  | 0.09 <sup>d</sup> | 312           |
| Zolmitriptan | 0.02 <sup>c</sup> | 1.80          |

\*Active pharmaceutical ingredients (APIs) with CNS related indications (excluding triptans as they primarily target the brain capillary vascular system)

<sup>a-h</sup> Each value calculated based on the literature data in [34], [35], [36], [37], [38], [39] and [40] respectively

respectively. The  $K_{m,app}$  of quinidine was 11.5  $\mu\text{M}$ , and the  $K_{m,app}$  for prazosin was 9.6  $\mu\text{M}$ . In literature, quinidine was previously reported with  $K_{m,app} = 13 \mu\text{M}$  in MDCKII-MDR1 cells [22], which is consistent with our result. In literature, the  $K_{m,app}$  data of prazosin was limited in MDCK studies, while  $K_{m,app} = 22 \mu\text{M}$  was reported in BCRP-expressing Caco-2 [23]. That indicates that the efflux transport of prazosin in Caco-2 cells is saturated at higher concentrations compared to BCRP-transfected MDCKII ZFN cells, likely due to the competing affinities from MDR1 and BCRP transporters in Caco-2.

Different strains of MDCK cells have been commonly seen in literature. For example, MDCKI and MDCKII were both derived from a parental cell line NBL-2, but isolated from low and high passage strains respectively [6]. Due to their cell line heterogeneity as well as culture conditions, the variability could be expected in the outcome of cell permeability assays [21]. In particular, long-time passaging of MDCK cells was found to alter cellular chromosome content, therefore the necessity for characterizing any drift of MDCK cells in culture was suggested [24]. Expression levels of efflux transporters were reported with dependence of cell passage [20, 25]. With ascending cell passage, transporter efficiency could be varied between lower and higher passaged cells, as the mRNA levels of transfected human transporter genes may be diminishing during the overexpression [20]. Therefore, we used lower and higher cell passages to investigate their influence on mRNA expression and efflux activities of individual transporters in MDCKII ZFN models. In our results, the mRNA level of hMDR1 or hBCRP from its each transfected MDCKII ZFN model was mildly enhanced at a higher passage, compared to a lower passage. ERs of quinidine and prazosin demonstrated a similar pattern of efflux transport activities from MDRI\_ZFN and BCRP\_ZFN models respectively, where the efflux activities were varied by cell passages applied. However, in our experience, the influence of cell passages on the displayed variability did not reach a point with diminishing efflux activities, which were commonly seen in recombinant cell models. More importantly, years of routine measurements of quality control substrates in permeability and efflux transport assays have substantiated the robustness and reliability of the MDCKII ZFN models.

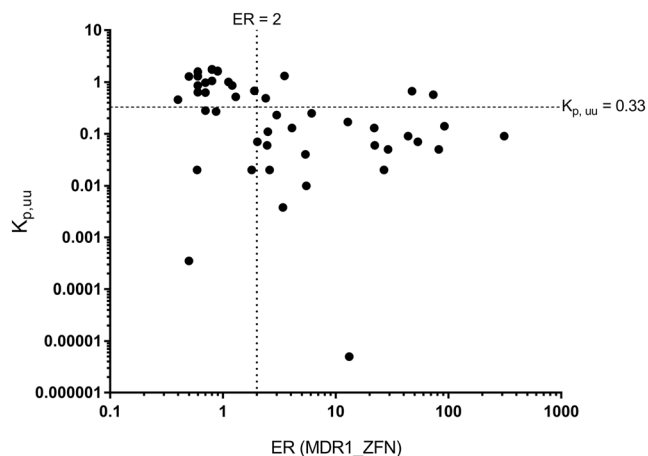


**Fig. 5** Correlation between  $K_{p,uu}$  and ER data for reference substances provided in Table III.  $K_{p,uu} = 0.33$  is used as a cutoff for identification of a brain penetrant, and  $ER = 2$  as a cutoff for efflux transport

Compared to MDCK cells, Caco-2 cells express relevant uptake and efflux transporters as in human gastrointestinal tract. Drug transport across Caco-2 cell monolayers was found to correlate well with *in vivo* bioavailability and absorption [26]. Especially, permeability of passive transport drugs in Caco-2 was reportedly comparable with human jejunum [27]. However, due to its different cell subpopulations, Caco-2 monolayer has variable expression of transporters, which may lead to uptake or efflux mechanistic interplay and subsequently under- or overpredict human situation [28]. Alternatively, selective inhibitors are used to ascertain the identity of responsible transporter, but off-target inhibition would factor in permeability assays and lead to false results [18]. Here, we used ZFN-mediated genetic knock-out Caco-2 models to assess MDR1 or BCRP-dependent substrate efflux transport.

Overall, most selected substrates were correctly categorized by both the double knock-out Caco-2 and MDCKII ZFN models. The two cell systems demonstrated good agreement over substrate identification, by using  $ER = 2$  as the cutoff for efflux transport. In detail, we demonstrated that MDR1\_Caco-2 and MDR1\_ZFN MDCKII displayed similar efflux levels for metoprolol or dantrolene (both  $ER < 2$ ) and amprenavir or vinblastine (both  $ER > 2$ ). However, rosuvastatin and sulfasalazine were only determined as a MDR1 substrate in MDR1\_Caco-2, but not in MDR1\_ZFN MDCKII. On the other hand, both BCRP\_Caco-2 and BCRP\_ZFN MDCKII were able to identify the metoprolol, amprenavir, fexofenadine, vinblastine with  $ER < 2$ , and the cimetidine, dantrolene, nitrofurantoin, rosuvastatin with  $ER > 2$ . Sulfasalazine was again determined as a BCRP substrate only in the Caco-2, but not in the MDCKII ZFN.

Indeed, discrepancy was observed in cases of rosuvastatin and sulfasalazine, for each inconsistent efflux properties between the double knock-out Caco-2 and MDCKII ZFN models. In our result, rosuvastatin was classified as a dual efflux substrate to both MDR1 and BCRP transporters in the knock-out Caco-2,

compared to only a BCRP substrate in BCRP\_ZFN MDCKII. These distinct efflux outcome was previously found in rosuvastatin studies with knock-down Caco-2 cells [29] and transfected MDCK cells [30]. In addition, sulfasalazine was classified as both MDR1 and BCRP substrate in the double knock-out Caco-2, but none in the MDCKII ZFN models. This was in agreement with a previous study with the NIH MDR-MDCK model, where efflux of sulfasalazine was also not mediated by either MDR1 or BCRP transporter [18]. Here, the inconsistent model predictability was presumably due to the lack of basolateral uptake transporters in MDCK cells, when compared to Caco-2 cells [31]. After all, the uptake of a substrate at the basolateral side of MDCK cells could be possibly “delayed”, and subsequently lead to ineffective efflux outcome. By contrast, Caco-2 cells express multiple transporters at both the apical and basolateral surfaces, and therefore are capable of active efflux of a “non-MDR1” or “non-BCRP” substrate [32]. In addition, passive diffusion properties of compounds could be another limiting factor for successful identification of efflux substrates. For example, sulfasalazine has a poor transcellular permeability at  $P_{app} < 1 \times 10^{-6}$  cm/s for basolateral to apical as well as apical to basolateral directions in WT\_ZFN cells. From the efflux-screening standpoint, poor cell penetration-mediated permeability could be a contributor of false negative result. Together, it highlights the importance of utilizing both Caco-2 and MDCK models during efflux and permeability assays to balance different model predictabilities and understand better “outlier” effects from efflux substrates.

One reliable quantitative assessment of compounds in brain penetration can be obtained by using the unbound brain to plasma partition coefficient  $K_{p,uu}$ . Using both internal and external  $K_{p,uu}$  dataset from 46 substances, the *in vitro* to *in vivo* correlation was applied against their respective ERs obtained in MDR1\_ZFN MDCKII cells. The *in vitro* MDCK result qualified approx. 80% of total reference substances (both true positive and true negative) with correct prediction of the brain penetration *in vivo*. The remaining 20% of test compounds were otherwise not predicted in the brain availability by the MDR1\_ZFN model, and potential reasons could be a slow concentration equilibration of compounds *in vivo* (false positive), limited brain tissue interaction (false positive), involvement of other efflux transporters like BCRP or MRP1–6 (false positive), specific brain uptake mechanism (false negative), or species differences (human vs. rodent; false positive and false negative). Previously, the Borst MDCKII-MDR1 cell line was compared with the NIH MDCKI-MDR1 over individual predictability for brain penetration [8]. The NIH model was reported with approx. 80% prediction rate and exceeded the Borst model at approx. 60% prediction rate, owing to higher abundance of human MDR1 expressed in the NIH cells. Although the MDR1\_ZFN cells were derived from Borst cells, the abundance of hMDR1 is higher compared to the original cell line [33], implicating the comparably higher predictive power. However, the set of test substances was

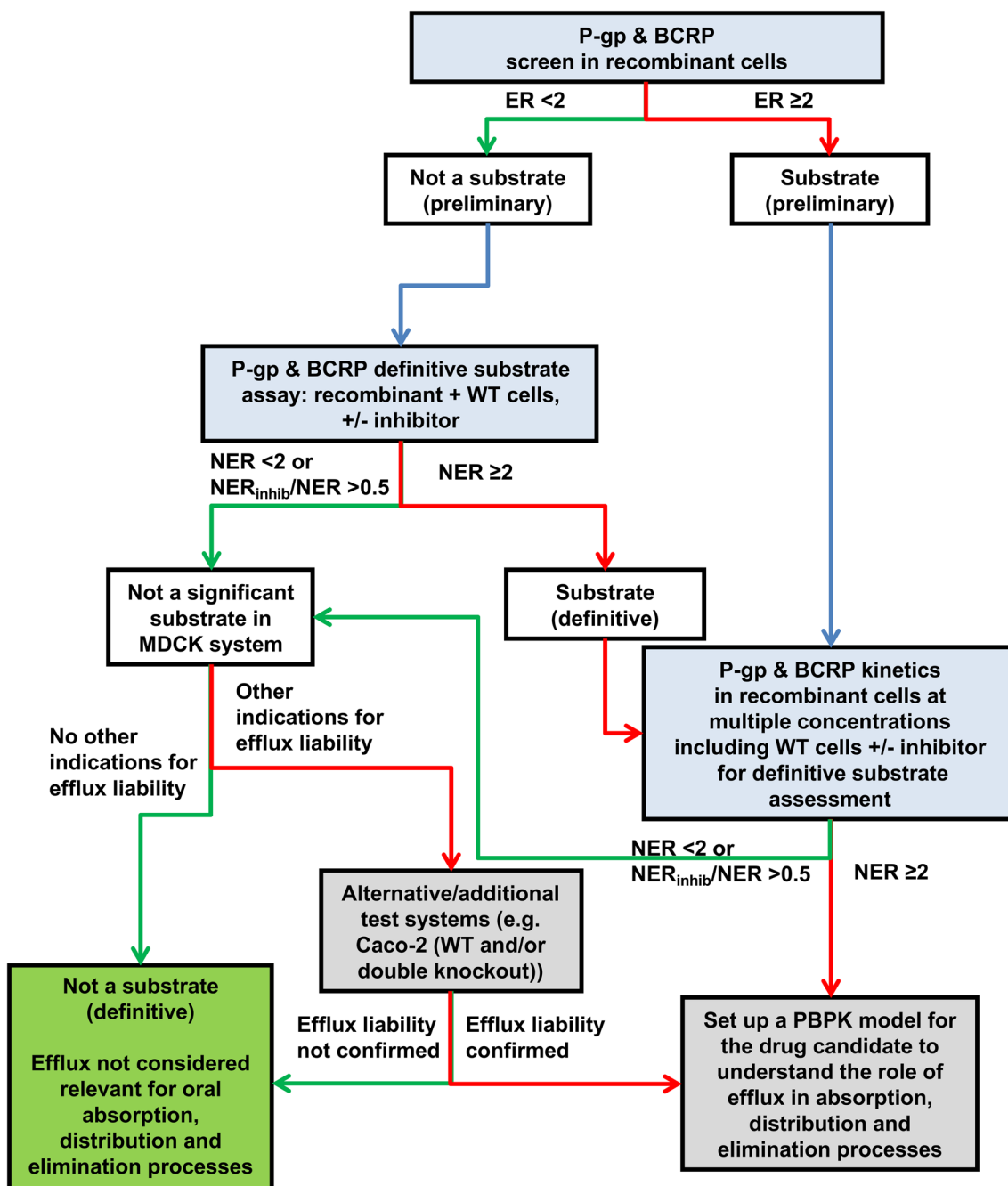


**Fig. 6** A screening procedure for characterization and identification of efflux transporter substrates. MDCKII ZFN cells are used as primary models for permeability and efflux transport assessment. Substrates with negative efflux liabilities are subject to counter-screening in additional systems, such as double knock-out Caco-2 cells

different, as well as that the predictability might alter for different substance classes. Therefore, continuous verification is necessary to maintain high reliability. In Table III, 20 active pharmaceutical ingredients (APIs) were highlighted, which have known CNS-related indications in human. 90% of them were predicted for brain availability by using ER and  $K_{p,uu}$  cut-off values. Exceptions were mainly covered by either of these two parameters in use or distinct substance properties. For example, carbamazepine and phenytoin, two antiepileptic

drugs, had a negative but borderline  $K_{p,uu}$  outcome ( $<0.33$ ), while their  $ER < 1$  values indicated positive brain availability. No brain penetration was predicted for the dopamine D2 receptor antagonist sulpiride *in vitro* and *in vivo*. Its suitability for the treatment of schizophrenia can be ascribed to the possibility of high dose regimes up to 1000 mg/d and the brain uptake mechanism *via* OCTs [41]. In addition, with  $K_{p,uu} = 0.25$  and  $ER = 6.12$  risperidone was predicted for a low brain availability, as reported in literature, where the brain entry of

risperidone was limited by P-gp *in vivo* [42]. Although risperidone is subject to efflux, it can be taken as an example, where efflux liability is not limiting its applicability as a CNS drug in general. However, a P-gp related risk must be considered.

Besides a therapeutic aspect, CNS-related side effects can be also in scope for the prediction of brain penetration. One example is H<sub>1</sub>-antihistamines when focusing on their indication as antiallergic drugs, where their central sedative properties are mostly undesirable. Here, more sedative 1st generation representatives including hydroxyzine, diphenhydramine and triprolidine could be predicted through ER and K<sub>p,uu</sub> for the CNS entry, however, both parameters also identified less sedative 2nd generation APIs, such as desloratadine, fexofenadine and cetirizine. Despite the 2nd generation derivative loratadine was identified as brain-available, it has an improved CNS side-effect profile, because it can be considered as a prodrug of the more potent and less brain-available desloratadine. All of these demonstrate that the identification of compounds for potential CNS treatment as well as for CNS related side effects and DDIs constitute integral parts of assessments for candidate selection in pharmaceutical drug development, which can be successfully addressed by *in vitro* ER screening using MDR1\_ZFN cells combined with additional *in vivo* assessment such as K<sub>p,uu</sub>.

Lastly, a screening method is outlined in Fig. 6 to provide an assay guideline for robust identification of efflux transporter substrates. In detail, MDCKII ZFN cell lines serve as primary models for evaluating drug candidates. Based on acquired ER values, compounds identified as substrates of either MDR1 or BCRP with a cutoff of ER ≥ 2 and NER ≥ 2 are investigated further to acquire kinetic parameters (i.e., K<sub>m</sub>, V<sub>max</sub>) in a concentration-dependent experiment. The intrinsic kinetic parameters are used for setting up a PBPK model for drug candidates to understand the role of efflux in absorption, distribution and elimination processes. Compounds that are not identified as efflux substrates but indicated with efflux liability, i.e., a low intrinsic passive permeability (P<sub>app</sub> < 1 × 10<sup>-6</sup> cm/s), should be further counter-screened in additional test systems, such as double knock-out Caco-2 models. If a candidate compound does not show efflux activity in Caco-2 either, efflux transport may not be considered relevant for oral absorption, distribution and elimination processes.

## CONCLUSION

The newly generated MDR1\_ZFN and BCRP\_ZFN MDCKII cell models have knock-down functional expression of endogenous cP-gp and were found reliable in identifying MDR1 and BCRP substrates in this study. Efflux ratio (ER) and next efflux ratio (NER) were two important parameters that would enable robust classification of efflux transporters, and with a cutoff of ER = 2/NER = 2, the predictability of

MDCKII ZFN models was overall consistent with relevant literature data. By assessing kinetic parameters in the MDCKII ZFN models, test substrates showed relatively good affinities with hMDR1 and hBCRP transporters, which was in line with literature reports. Cell passage showed mild influence on mRNA levels of efflux transporters as well as their functional activities in the MDCKII ZFN models. However, the ER variability could be controlled *via* routine applications of quality control substrates in permeability and efflux transport assays.

Sporadically, the MDCKII ZFN cells may classify efflux substrates inconsistently, due to potential species differences from expressed uptake or efflux transporters, when compared to human gastrointestinal models. Double knock-out Caco-2 models were herein introduced as references to counter-screen substrates from MDCKII ZFN studies. A majority of MDR1 and BCRP substrates were successfully identified with the models of two species, at the levels of hMDR1 and hBCRP-mediated efflux transport. The discrepancy exhibited by MDR1\_ZFN and BCRP\_ZFN MDCKII cells was overall limited as compared to the Caco-2 models, and the result was comparable with the literature.

In prediction of brain penetration, MDR1\_ZFN MDCKII model could serve as a useful tool to accurately correlate its ERs with *in vivo* K<sub>p,uu</sub> data. Eighty percent of all test compounds could be correctly predicted for their outcome in brain exposure.

Considering all these findings, we conclude that MDR1\_ZFN and BCRP\_ZFN MDCKII models can produce robust results for permeability and efflux transporter assays, adequately identify MDR1 and BCRP substrates, and more importantly serve as useful tools for prediction of brain penetration.

## ACKNOWLEDGEMENT

The authors would like to thank Juliane Hoeckels-Messemer, Sylvia Hellwig and Patricia Muschong of AbbVie for their technical support.

**Disclosures** Dong Ye, Manuel Weinheimer, Loic Laplanche, Mario Mezler are employees of AbbVie and may own AbbVie stock. Zhizhou Fang was an employee of AbbVie at the time when he contributed to the work being discussed, and he currently works at Merck Healthcare KGaA, Germany. Anna Harder was a master student of AbbVie for this work at the time and currently works at Braun Melsungen AG, Germany. The design, study conduct, and financial support for this research was provided by AbbVie. AbbVie participated in the interpretation of data, review, writing and approval of the publication. All authors declare no competing financial interest in this work.

All authors contributed to the study conception and design. Material preparation, data collection and analysis were performed by Dong Ye, Anna Harder, Zhizhou Fang. The first draft of the manuscript was written by Dong Ye and all authors commented on previous versions of the manuscript. All authors actively contributed to the final text, read and approved the final manuscript.

## REFERENCES

- Guidance for Industry: *In Vitro* Metabolism and Transporter Mediated Drug-Drug Interaction Studies. 2017. <https://www.fda.gov/media/108130/download>.
- Hellinger É, Veszélka S, Tóth AE, Walter F, Kittel Á, Bakk ML, et al. Comparison of brain capillary endothelial cell-based and epithelial (MDCK-MDR1, Caco-2, and VB-Caco-2) cell-based surrogate blood-brain barrier penetration models. *Eur J Pharm Biopharm*. 2012;82(2):340–51.
- Garberg P, Ball M, Borg N, Cecchelli R, Fenart L, Hurst R, et al. *In vitro* models for the blood-brain barrier. *Toxicol in Vitro*. 2005;19(3):299–334.
- Sai Y, Tsuji A. Transporter-mediated drug delivery: recent progress and experimental approaches. *Drug Discov Today*. 2004;9(16):712–20.
- Sampson KE, Brinker A, Pratt J, Venkatraman N, Xiao Y, Blasberg J, et al. Zinc finger nuclease-mediated gene knockout results in loss of transport activity for P-glycoprotein, BCRP, and MRP2 in Caco-2 cells. *Drug Metab Dispos*. 2015;43(2):199–207.
- Dukes JD, Whitley P, Chalmers AD. The MDCK variety pack: choosing the right strain. *BMC Cell Biol*. 2011;12:43.
- Kikuchi R, de Moraes SM, Kalvass JC. *In vitro* P-glycoprotein efflux ratio can predict the *in vivo* brain penetration regardless of biopharmaceutics drug disposition classification system class. *Drug Metab Dispos*. 2013;41(12):2012–7.
- Feng B, West M, Patel NC, Wager T, Hou X, Johnson J, et al. Validation of human MDR1-MDCK and BCRP-MDCK cell lines to improve the prediction of brain penetration. *J Pharm Sci*. 2019;108:2476–83.
- Feng B, Doran AC, Di L, West MA, Osgood SM, Mancuso JY, et al. Prediction of human brain penetration of P-glycoprotein and breast cancer resistance protein substrates using *in vitro* transporter studies and animal models. *J Pharm Sci*. 2018;107(8):2225–35.
- Sato S, Tohyama K, Kosugi Y. Investigation of MDR1-overexpressing cell lines to derive a quantitative prediction approach for brain disposition using *in vitro* efflux activities. *Eur J Pharm Sci*. 2019;105:119.
- Gartzke D, Delzer J, Laplanche L, Uchida Y, Hoshi Y, Tachikawa M, et al. Genomic knockout of endogenous canine P-glycoprotein in wild-type, human P-glycoprotein and human BCRP transfected MDCKII cell lines by zinc finger nucleases. *Pharm Res*. 2015;32(6):2060–71.
- Simoff I, Karlgren M, Backlund M, Lindström A-C, Gaugaz FZ, Matsson P, et al. Complete knockout of endogenous Mdr1 (Abcb1) in MDCK cells by CRISPR-Cas9. *J Pharm Sci*. 2016;105(2):1017–21.
- Karlgrén M, Simoff I, Backlund M, Wegler C, Keiser M, Handin N, et al. A CRISPR-Cas9 generated MDCK cell line expressing human MDR1 without endogenous canine MDR1 (cABCB1): an improved tool for drug efflux studies. *J Pharm Sci*. 2017;106(9):2909–13.
- Chen EC, Broccatelli F, Plise E, Chen B, Liu L, Cheong J, et al. Evaluating the utility of canine Mdr1 knockout Madin-Darby canine kidney I cells in permeability screening and efflux substrate determination. *Mol Pharm*. 2018;15(11):5103–13.
- Saeki T, Ueda K, Tanigawara Y, Hori R, Komano T. P-glycoprotein-mediated transcellular transport of MDR-reversing agents. *FEBS Lett*. 1993;324(1):99–102.
- Polli JW, Wring SA, Humphreys JE, Huang L, Morgan JB, Webster LO, et al. Rational use of *in vitro* P-glycoprotein assays in drug discovery. *J Pharmacol Exp Ther*. 2001;299(2):620–8.
- Haslam IS, Jones K, Coleman T, Simmons N. Induction of P-glycoprotein expression and function in human intestinal epithelial cells (T84). *Biochem Pharmacol*. 2008;76(7):850–61.
- Wang Q, Strab R, Kardos P, Ferguson C, Li J, Owen A, et al. Application and limitation of inhibitors in drug-transporter interactions studies. *Int J Pharm*. 2008;356(1–2):12–8.
- Sane R, Agarwal S, Mittapalli RK, Elmquist WF. Saturable active efflux by p-glycoprotein and breast cancer resistance protein at the blood-brain barrier leads to nonlinear distribution of elacridar to the central nervous system. *J Pharmacol Exp Ther*. 2013;345(1):111–24.
- Wang Z, Pal D, Patel A, Kwatra D, Mitra AK. Influence of over-expression of efflux proteins on the function and gene expression of endogenous peptide transporters in MDR-transfected MDCKII cell lines. *Int J Pharm*. 2013;441(1–2):40–9.
- Volpe DA. Variability in Caco-2 and MDCK cell-based intestinal permeability assays. *J Pharm Sci*. 2008;97(2):712–25.
- Heikkinen AT, Korjamo T, Lepikkö V, Mönkkönen J. Effects of experimental setup on the apparent concentration dependency of active efflux transport in *in vitro* cell permeation experiments. *Mol Pharm*. 2010;7(2):605–17.
- Wright JA, Haslam IS, Coleman T, Simmons NL. Breast cancer resistance protein BCRP (ABCG2)-mediated transepithelial nitrofurantoin secretion and its regulation in human intestinal epithelial (Caco-2) layers. *Eur J Pharmacol*. 2011;672(1–3):70–6.
- Cassio D. Long term culture of MDCK strains alters chromosome content. *BMC Res Notes*. 2013;6(1):162.
- Lewin B. *Genes IV*. Am J Phys Anthropol. New York: Oxford University Press; 1990.
- Artursson P, Karlsson J. Correlation between oral drug absorption in humans and apparent drug permeability coefficients in human intestinal epithelial (Caco-2) cells. *Biochem Biophys Res Commun*. 1991;175(3):880–5.
- Lennerhäls H, Palm K, Fagerholm U, Artursson P. Comparison between active and passive drug transport in human intestinal epithelial (Caco-2) cells *in vitro* and human jejunum *in vivo*. *Int J Pharm*. 1996;127(1):103–7.
- Larregieu CA, Benet LZ. Drug discovery and regulatory considerations for improving *in silico* and *in vitro* predictions that use Caco-2 as a surrogate for human intestinal permeability measurements. *AAPS J*. 2013;15(2):483–97.
- Li J, Volpe DA, Wang Y, Zhang W, Bode C, Owen A, et al. Use of transporter knockdown Caco-2 cells to investigate the *in vitro* efflux of statin drugs. *Drug Metab Dispos*. 2011;39(7):1196–202.
- Huang L, Wang Y, Grimm S. ATP-dependent transport of rosuvastatin in membrane vesicles expressing breast cancer resistance protein. *Drug Metab Dispos*. 2006;34(5):738–42.
- Li J, Wang Y, Zhang W, Huang Y, Hein K, Hidalgo JJ. The role of a basolateral transporter in rosuvastatin transport and its interplay with apical breast cancer resistance protein in polarized cell monolayer systems. *Drug Metab Dispos*. 2012;40(11):2102–8.
- Hirohashi T, Suzuki H, Chu X-Y, Tamai I, Tsuji A, Sugiyama Y. Function and expression of multidrug resistance-associated protein family in human colon adenocarcinoma cells (Caco-2). *J Pharmacol Exp Ther*. 2000;292(1):265–70.
- Gartzke D, Fricker G. Establishment of optimized MDCK cell lines for reliable efflux transport studies. *J Pharm Sci*. 2014;103(4):1298–304.

34. Schinkel AH, Wagenaar E, van Deemter L, Mol C, Borst P. Absence of the *mdr1a* P-Glycoprotein in mice affects tissue distribution and pharmacokinetics of dexamethasone, digoxin, and cyclosporin A. *J Clin Invest*. 1995;96(4):1698–705.
35. Van Asperen J, Schinkel AH, Beijnen JH, Nooijen WJ, Borst P, van Tellingen O. Altered pharmacokinetics of vinblastine in *Mdr1a* P-glycoprotein-deficient mice. *JNCI: J Natl Cancer Inst*. 1996;88(14):994–9.
36. Evans DC, O'Connor D, Lake BG, Evers R, Allen C, Hargreaves R. Eletriptan metabolism by human hepatic CYP450 enzymes and transport by human P-glycoprotein. *Drug Metab Dispos*. 2003;31(7):861–9.
37. Schinkel A, Smit J, Van Tellingen M, Beijnen J, Wagenaar E, Van Deemter L, et al. Disruption of the mouse *mdr1a* P-glycoprotein gene leads to a deficiency in the blood-brain barrier and to increased sensitivity to drugs. *Cell*. 1994;77(4):491–502.
38. Kemper EM, Cleypool C, Boogerd W, Beijnen JH, van Tellingen O. The influence of the P-glycoprotein inhibitor zosuquidar trihydrochloride (LY335979) on the brain penetration of paclitaxel in mice. *Cancer Chemother Pharmacol*. 2004;53(2):173–8.
39. Kusuvara H, Suzuki H, Terasaki T, Kakee A, Lemaire M, Sugiyama Y. P-glycoprotein mediates the efflux of quinidine across the blood-brain barrier. *J Pharmacol Exp Ther*. 1997;283(2):574–80.
40. Hendrikse N, Schinkel A, De Vries E, Fluks E, Van der Graaf W, Willemsen A, et al. Complete *in vivo* reversal of P-glycoprotein pump function in the blood-brain barrier visualized with positron emission tomography. *Br J Pharmacol*. 1998;124(7):1413–8.
41. Pereira JNDS, Tadjerpisheh S, Abed MA, Saadatmand AR, Weksler B, Romero IA, et al. The poorly membrane permeable antipsychotic drugs amisulpride and sulpiride are substrates of the organic cation transporters from the SLC22 family. *AAPS J*. 2014;16(6):1247–58.
42. Wang J-S, Ruan Y, Taylor RM, Donovan JL, Markowitz JS, DeVane CL. The brain entry of risperidone and 9-hydroxyrisperidone is greatly limited by P-glycoprotein. *Int J Neuropsychopharmacol*. 2004;7(4):415–9.

**Publisher's Note** Springer Nature remains neutral with regard to jurisdictional claims in published maps and institutional affiliations.